

# Consensus recommendations for MRI and PET imaging of primary central nervous system lymphoma: guideline statement from the International Primary CNS Lymphoma Collaborative Group (IPCG)

Ramon F. Barajas Jr,<sup>†</sup> Letterio S. Politi,<sup>°</sup> Nicoletta Anzalone,<sup>°</sup> Heiko Schöder,<sup>°</sup> Christopher P. Fox, Jerrold L. Boxerman, Timothy J. Kaufmann, C. Chad Quarles, Benjamin M. Ellingson,<sup>°</sup> Dorothee Auer, Ovidiu C. Andronesi, Andres J. M. Ferreri, Maciej M. Mrugala, Christian Grommes, Edward A. Neuwelt, Prakash Ambady, James L. Rubenstein, Gerald Illerhaus, Motoo Nagane,<sup>°</sup> Tracy T. Batchelor, and Leland S. Hu<sup>†</sup>

*Department of Radiology, Neuroradiology Section, Oregon Health & Science University, Portland Oregon, USA (R.F.B.); Advanced Imaging Research Center, Oregon Health & Science University, Portland, Oregon, USA (R.F.B.); Knight Cancer Institute Translational Oncology Program, Oregon Health & Science University, Portland, Oregon, USA (R.F.B.); Humanitas University and Humanitas Research and Clinical Center - IRCCS, Milan, Italy (L.S.P.); Boston Children's Hospital, Boston, Massachusetts, USA (L.S.P.); Neuroradiology Unit, IRCCS San Raffaele Hospital and Vita-Salute University, Milan, Italy (N.A.); Department of Radiology, Memorial Sloan Kettering Cancer Center, New York, New York, USA (H.S.); Department of Clinical Haematology, Nottingham University Hospitals NHS Trust, School of Medicine, University of Nottingham, Nottingham, UK (C.P.F.); Department of Diagnostic Imaging, Warren Alpert Medical School, Brown University, Providence, Rhode Island, USA (J.L.B.); Department of Radiology, Mayo Clinic, Rochester, Minnesota, USA (T.J.K.); Department of Neuroimaging Research & Barrow Neuroimaging Innovation Center, Barrow Neurological Institute, Phoenix, Arizona, USA (C.C.Q.); UCLA Brain Tumor Imaging Laboratory (BTIL), Departments of Radiological Sciences and Psychiatry, David Geffen School of Medicine, University of California - Los Angeles, Los Angeles, California, USA (B.M.E.); Departments of Radiological Sciences, Psychiatry, and Biobehavioral Sciences, David Geffen School of Medicine, University of California - Los Angeles, Los Angeles, California, USA (B.M.E.); Versus Arthritis Pain Centre, University of Nottingham, Nottingham, UK (D.A.); NIHR Nottingham Biomedical Research Centre, Queen's Medical Centre, University of Nottingham, Nottingham, UK (D.A.); Sir Peter Mansfield Imaging Centre, School of Medicine, University of Nottingham, Nottingham, UK (D.A.); A. A. Martinos Center for Biomedical Imaging, Department of Radiology, Massachusetts General Hospital, Charlestown, Massachusetts, USA (O.C.A.); Lymphoma Unit, Department of Onco-Hematology, IRCCS San Raffaele Scientific Institute, Milan, Italy (A.J.M.F.); Department of Medicine, Division of Hematology and Oncology, Mayo Clinic Cancer Center, Phoenix, Arizona, USA (M.M.M.); Department of Neurology, Mayo Clinic, Phoenix, Arizona, USA (M.M.M.); Department of Neurology, Memorial Sloan Kettering Cancer Center, New York, New York, USA (C.G.); Department of Neurology, Weill Cornell Medical School, New York, New York, USA (C.G.); Blood-Brain Barrier Program, Oregon Health & Science University, Portland, Oregon, USA (E.A.N., P.A.); Department of Neurology, Oregon Health & Science University, Portland, Oregon, USA (E.A.N., P.A.); Department of Neurological Surgery, Oregon Health & Science University, Portland, Oregon, USA (E.A.N.); Portland Veterans Affairs Medical Center, Portland, Oregon, USA (E.A.N.); Division of Hematology/Oncology, University of California, San Francisco, California, USA (J.L.R.); Department of Medicine, University of California, San Francisco, California, USA (J.L.R.); Helen Diller Family Comprehensive Cancer Center, University of California, San Francisco, California, USA (J.L.R.); Clinic of Hematology, Oncology and Palliative Care, Klinikum Stuttgart, Stuttgart, Germany (G.I.); Department of Neurosurgery, Kyorin University Faculty of Medicine, Tokyo, Japan (M.N.); Department of Neurology, Brigham and Women's Hospital, Harvard Medical School, Boston, Massachusetts, USA (T.T.B.); Department of Radiology, Neuroradiology Division, Mayo Clinic, Phoenix, Arizona, USA (L.S.H.)*

<sup>†</sup>Indicated co-corresponding authors.

**Corresponding Authors:** Ramon F. Barajas, Jr. MD, Associate Professor, Neuroradiology Section, Department of Radiology, Advanced Imaging Research Center, Knight Cancer Institute, 3181 S.W. Sam Jackson Park Rd., Portland, OR 97239, USA ([barajaslab@ohsu.edu](mailto:barajaslab@ohsu.edu)); Leland S. Hu, MD, Neuroradiology Division, Department of Radiology, Consultant, Mayo Clinic Arizona, Associate Professor of Radiology, Mayo Clinic College of Medicine, 5777 E. Mayo Blvd, Phoenix, AZ 85054, USA ([hu.leland@mayo.edu](mailto:hu.leland@mayo.edu)).

## Abstract

Advanced molecular and pathophysiologic characterization of primary central nervous system lymphoma (PCNSL) has revealed insights into promising targeted therapeutic approaches. Medical imaging plays a fundamental role in PCNSL diagnosis, staging, and response assessment. Institutional imaging variation and inconsistent clinical trial reporting diminishes the reliability and reproducibility of clinical response assessment. In this context, we aimed to: (1) critically review the use of advanced positron emission tomography (PET) and magnetic resonance imaging (MRI) in the setting of PCNSL; (2) provide results from an international survey of clinical sites describing the current practices for routine and advanced imaging, and (3) provide biologically based recommendations from the International PCNSL Collaborative Group (IPCG) on adaptation of standardized imaging practices. The IPCG provides PET and MRI consensus recommendations built upon previous recommendations for standardized brain tumor imaging protocols (BTIP) in primary and metastatic disease. A biologically integrated approach is provided to address the unique challenges associated with the imaging assessment of PCNSL. Detailed imaging parameters facilitate the adoption of these recommendations by researchers and clinicians. To enhance clinical feasibility, we have developed both “ideal” and “minimum standard” protocols at 3T and 1.5T MR systems that will facilitate widespread adoption.

## Introduction

### Statement of Need

Primary central nervous system lymphoma (PCNSL) represents a rare but aggressive form of extra-nodal non-Hodgkin lymphoma preferentially affecting the brain, spinal cord, cerebrospinal fluid (CSF), cranial and spinal nerves, and vitreoretinal compartment. The WHO classification of lymphoid neoplasm recognizes this distinct entity as primary diffuse large B-cell lymphoma of the central nervous system (CNS), representing the overwhelming majority of PCNSL. Recent advances in molecular and pathophysiologic characterization of PCNSL have expanded our understanding of the biologic etiology of this malignancy and have offered novel insights into targeted therapeutics. As treatment paradigms become more complex, the clinical tools for disease evaluation must also evolve. As a prime example, magnetic resonance imaging (MRI) plays a fundamental role in the clinical diagnosis, staging, and response assessment of PCNSL in immunocompetent patients. But while MRI can characterize an array of tumor phenotypes, only a limited subset of MRI features are routinely used: (1) T1W contrast enhancement (CE) as a measure of blood-brain barrier (BBB) disruption and tumor burden; and (2) T2W signal as a measure of vasogenic edema beyond MRI enhancement. Meanwhile, the past decade has witnessed increasing assimilation of a broader panel of advanced MRI techniques that provide uniquely complementary information about tumor biology, including regional differences in bulk water movement on diffusion-weighted imaging (DWI), quantitative assessment of vascular leakage on dynamic contrast-enhanced (DCE)-MRI, and microvessel volume and proliferation on dynamic susceptibility contrast perfusion MRI (DSC-MRI) (Figure 1). Additionally, volumetric measurements have recently been advocated in glioma and metastases to provide

more quantitative and reproducible biomarkers for staging and response assessment. While routine volumetric analysis of tumor size remains clinically challenging, the acquisition of 3D volumetric sequences may facilitate the development of reliable methodology. Extending these advanced applications to the setting of PCNSL offers the potential to bridge important clinical gaps. In this context, the goals of this paper are: (1) to provide a critical review of the use of advanced MRI techniques and analyses in the setting of PCNSL; (2) to provide results from an international survey of clinical sites in regard to their current imaging practices for routine and advanced imaging, and (3) to provide recommendations from the International PCNSL Collaborative Group (IPCG) on adaptation of standard imaging practices for future use in clinical trials and in clinical practice. The adoption of a standardized, evidence-based, imaging technique by teams caring for patients with PCNSL is expected to ultimately lead to improved clinical therapeutic response assessment and clinical outcomes.

### Epidemiology

In immunocompetent patients, PCNSL comprises approximately 4% of all intracranial neoplasms and 4%-6% of all extra-nodal lymphomas.<sup>1</sup> With an incidence of 0.5 patients per 100 000 per year, increasing incidence of PCNSL has been recognized in recent years, particularly in older patients (>60 years). Unlike other brain tumors, PCNSL responds favorably to both chemotherapy and radiation therapy, and the widespread adoption of high-dose methotrexate (MTX) has improved outcomes over recent decades.<sup>2</sup> Notwithstanding the substantial clinical progress, survival remains inferior compared with lymphomas outside the CNS. Only half of the patients experience durable remissions, and the prognosis of those patients with non-response to first-line therapy remains dismal.<sup>2</sup>

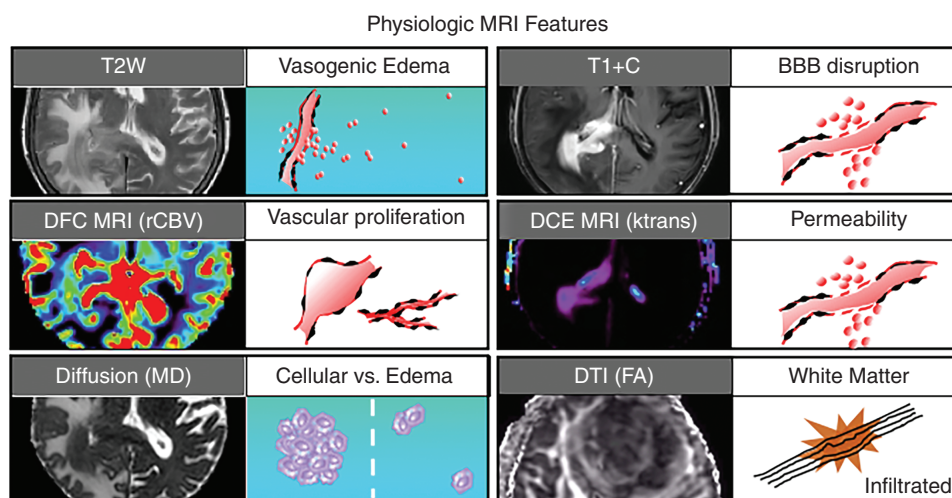


**Fig. 1** Biophysical features characterized by conventional and advanced physiologic MRI techniques. Shown are 6 MRI techniques that are commonly employed in neuro-oncologic imaging, along with their respective corresponding tumor phenotypes. T2-weighted (T2W) signal is typically used to define vasogenic edema. T1-weighted post-contrast enhancement (T1 + C) shows areas of disrupted blood-brain barrier (BBB). Dynamic susceptibility contrast (DSC) MRI measures of relative cerebral blood volume (rCBV) define microvascular volume as an indicator of tumor-related angiogenesis. Dynamic contrast-enhanced (DCE) MRI measures of vascular permeability ( $K^{\text{trans}}$ ). Diffusion-weighted imaging apparent diffusion coefficient (ADC) correlates with cellular density and proliferative indices and can aid in distinguishing tumor from vasogenic edema. Diffusion tensor imaging (DTI) fractional anisotropy (FA) measures the integrity of white matter tracts, which can be used to identify regions of tumor infiltration.

### Current Standards for PCNSL Imaging and Associated Clinical Challenges

**Conventional T1-weighted contrast-enhanced MRI.**—Gadolinium T1-weighted contrast-enhanced magnetic resonance imaging (CE-MRI) plays an integral role in non-invasive diagnosis and therapeutic monitoring of PCNSL. By convention, tumor burden has been defined by measuring the sum product diameter of abnormal CE on T1W images (T1 + C), which represents leakiness of the disrupted BBB. Current IPCG response assessment recommendations in part rely upon CE-MRI for the establishment of baseline disease and evaluation of therapeutic response.<sup>3</sup> Following therapy, current recommendations for imaging-based response assessment rely on enhancement characteristics for all PCNSL patients in clinical practice and in clinical trials.

**Challenges of using two-dimensional sum product measurements of tumor burden.**—At initial diagnosis, PCNSL in immunocompetent hosts classically demonstrates avidly enhancing lesions (up to 60%-75% of which are multiple). Most are supratentorial (80%), in a periventricular or deep cerebral white matter distribution. As shown in [Figure 2](#), both morphology and multiplicity of MRI-enhancing lesions can present difficulties in applying conventional two-dimensional (2D) sum product measurements, both in regard to labor intensiveness and inter-user variability. This can present challenges for reliably defining simple and reproducible measures of tumor burden at baseline, and response assessment based on serial

imaging. In this way, the volumetric analysis would help to automate measurements of tumor burden, with improved precision and clinical applicability.<sup>4,5</sup>

**Variations in MRI acquisition parameters can influence the degrees of enhancement.**—Variation in MRI sequence parameters, as well as timing and dosage of MRI contrast administration, affect the degrees of CE, and therefore the imaging measurements of tumor burden and response assessment.<sup>4-6</sup> Unfortunately, data on MRI sequence parameters and timing of contrast administration in PCNSL are limited. Given the current lack of reported MRI sequence parameters, it must be assumed that clinical trials of PCNSL utilized MRI techniques available to them at the time of study conduct. Studies before 2010 are likely to have utilized thick-sliced (3-5 mm) 2D spin-echo (SE) techniques on 1.5T field strength magnets. More recent studies may have used higher resolution thin-sliced (<2 mm) three-dimensional (3D) gradient-echo (GE) techniques on 3T field strength magnets. The use of higher resolution and field strength techniques have been shown to improve the detection of small enhancing foci.<sup>5</sup> Current treatment paradigms rely upon the accurate assessment of baseline and subsequent follow-up changes in contrast-enhancing lesion size. Therefore, a widely reproducible imaging approach for accurately determining lesion enhancement is of the utmost clinical importance. While post-processing techniques can help offset some of these variabilities, most efforts to develop standardized imaging have focused on consensus protocols for image acquisition.

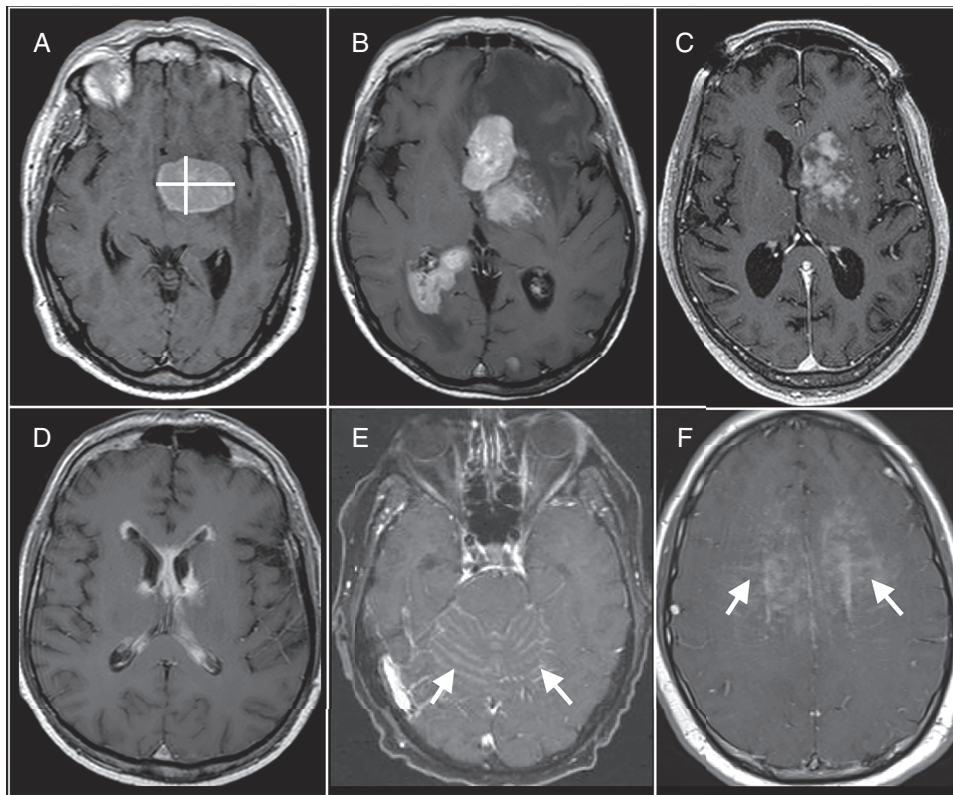


**Fig. 2** Challenges of bidirectional measurements of primary central nervous system lymphoma (PCNSL) tumor burden. (A) A single-rounded PCNSL mass lends itself to straightforward bidirectional measurement (yellow lines). (B) These bidirectional measurements can also be applied to multiple discrete masses. However, bidirectional measurements become more challenging with varied imaging patterns, such as with (C) heterogeneous enhancement, (D) linear ependymal enhancement, (E) leptomeningeal enhancement (arrows), and (F) linear perivascular enhancement (arrows). These varied imaging patterns would be more amenable to measurement using volumetric-based approaches to define tumor burden. Abbreviations: ADC, apparent diffusion coefficient; CBV, cerebral blood volume; DCE, dynamic contrast-enhanced; DSC, dynamic susceptibility contrast; PCNSL, primary central nervous system lymphoma.

**Assessment of non-enhancing tumor burden.**—PCNSL is known to be an infiltrative disease. The likelihood of disease burden extending beyond the segment of BBB disruption, into the non-enhancing signal abnormality on T2W images, is supported by data on clinical mortality following gross total resection of MRI enhancement, as well as treatment failure related to BBB impenetrable drug agents. In general, there is a paucity of data on the use of T2-weighted signal in response assessment of PCNSL. While a minority of cases demonstrate predominant non-enhancing disease relapse, it is a clinically important imaging variant that should be recognized and given consideration in the consensus recommendations.<sup>7–11</sup> T2W and fluid-attenuated inversion-recovery (FLAIR) sequences are sensitive but often nonspecific for the detection of disease. Despite T2-weighted FLAIR being heavily T2-weighted, there are some degrees of T1 effect that can be detected following the administration of gadolinium contrast.<sup>12</sup> Thus, contrast-enhanced T2-weighted FLAIR (CE-T2W-FLAIR) has shown promise in the detection of neoplastic foci.<sup>7–11</sup>

**Distinguishing tumor relapse from posttreatment-related effects.**—High-dose MTX remains the backbone

of PCNSL therapy. However, there is emerging interest in evaluating biologically specific therapies, especially in the refractory or recurrent setting. Recent advancements in understanding the neuro-immune landscape and success of immune check-point therapeutic blockade of systemic cancers have paved the way for ongoing clinical trials of targeted immunotherapeutics in PCNSL (NCT:02857426, and NCT:02779101).<sup>13,14</sup> Other novel agents targeting Bruton tyrosine kinase, interferon regulatory factor 4, phosphatidylinositol-4,5-bisphosphate 3-kinase and mammalian target of rapamycin are also being undertaken.<sup>15</sup> The possibility of early radiologic progression by traditional response assessment criteria due to treatment-related local immune response may result in unexpected challenges in interpreting the significance of persisting MRI enhancement following therapy; which remains a common clinical dilemma.<sup>16,17</sup> Specifically, the uncertainty of delineating complete response (CR) from unconfirmed (CRu) or partial response (PR), can have important prognostic and therapeutic implications; for example, the presence of residual disease following stem cell transplantation would be a potential indication for whole brain radiation therapy (WBRT).<sup>3</sup> Additionally, in cancer centers without dedicated

Neuroradiology expertise, stable persisting lesions observed with CRu may be erroneously classified as residual disease. The use of advanced techniques in other brain tumors, such as glioma, offers proof of concept for the application of advanced techniques, such as DSC perfusion MRI, to help improve the specificity of diagnosis. As an example, the use of DSC perfusion MRI in glioma has been used to distinguish tumor recurrence from treatment-related effects such as pseudoprogression or radiation necrosis.<sup>18,19</sup> While the phenomenon of pseudoprogression itself is rare in PCNSL treated conventionally, this phenomenon may become more relevant in PCNSL with newer immunotherapeutic agents with differing modes of action.<sup>20</sup>

### Clinical Applications of Advanced Physiologic Imaging in PCNSL

**Diffusion-weighted MRI.**—DWI is a widely utilized non-contrast MRI sequence for the clinical assessment of patients with PCNSL. Two *b* values (effect measure of water diffusion strength), such as 0 and 1000 s/mm<sup>2</sup>, are often obtained, and a mono-exponential fit of the observed signal decay allows for the generation of an apparent diffusion coefficient (ADC) value. Of note, for accuracy of ADC calculation, recent brain tumor imaging protocol (BTIP) consensus recommendations have suggested the use of three *b* values; 0, 500, and 1000 s/mm<sup>2</sup>. The ADC value is the most commonly used quantitative DWI metric. ADC is sensitive to microscopic diffusion of unbound extracellular water molecules.<sup>21</sup> As such, the reduction of water diffusion within the tumor extracellular space comprised of densely packed proliferating cells can be noninvasively characterized with MRI.<sup>21,22</sup>

Hypercellularity and a high proliferation index are characteristic biological features of PCNSL. Previous studies have reported that ADC values inversely correlate with histopathologic assessment of PCNSL cellular density and may be predictive of clinical outcomes.<sup>22,23</sup> Some retrospective studies have suggested that pre-therapeutic ADC measurements within the contrast-enhancing lesion are predictive of PFS (progression-free survival) and OS (overall survival) in immunocompetent patients undergoing combined high-dose MTX and rituximab therapy.<sup>23,24</sup> When applied to a pilot immunochemotherapy study with high-dose MTX, temozolomide, and rituximab followed by consolidation with etoposide and high-dose cytarabine, it is suggested that ADC values may provide useful predictive information on outcome vs established clinical indices.<sup>25</sup>

ADC values are also clinically useful in the differentiation of PCNSL from other primary brain tumors as ADC values within PCNSL are significantly lower when compared to glioblastoma.<sup>22</sup> This suggests that the high degrees of cellularity can be useful in the diagnostic assessment of PCNSL (Figure 3). Additionally, the combined diagnostic performance of PCNSL CSF biomarkers (CXCL-13 and IL-10) and ADC is superior to the use of any single biomarker.<sup>26</sup>

**Dynamic susceptibility contrast perfusion MRI.**—Over the past decade, DSC-MRI emerged as a clinically valuable

and accessible tool in neuro-oncology. The DSC-MRI technique measures relative cerebral blood volume (rCBV) as a surrogate noninvasive imaging biomarker of tissue microvascular volume.<sup>27,28</sup> rCBV assessment may be of clinical utility for PCNSL diagnosis and clinical outcomes.<sup>24,29</sup> The observation that rCBV may be of predictive value is consistent with the reported histological observations. Takeuchi et al. have demonstrated that patients with lymphoma with elevated vascular endothelial growth factor (VEGF) expression and microvascular density counts had prolonged OS.<sup>30</sup> Future studies are needed to apply rCBV for other potential applications, including characterization of disease burden, molecular stratification, and contribution to response assessment.

Assessment of rCBV has also been shown to be clinically useful in the pre-operative differentiation of PCNSL from glioblastoma. The literature suggests that PCNSL rCBV values, while somewhat variable, nonetheless are lower than those observed within glioblastoma (Figure 3).<sup>31</sup> This difference may aid in the clinical diagnosis of PCNSL and suggests that a fundamentally distinct biological process is occurring. Unlike glioblastoma, PCNSL neoangiogenesis does not result in marked degrees of microvascular proliferation or microvascular glomeruloid dilation. Histological and electron microscopy of PCNSL microvasculature suggests that only a minority of tumors demonstrate neoangiogenesis that lacks a neurovascular unit.

**Dynamic contrast-enhanced (DCE) perfusion MRI.**—DCE-MRI captures unique features of the vascular microenvironment including BBB permeability, making it a candidate to characterize lymphomas and other brain tumors, in the differential diagnosis, response assessment, and survival analysis.<sup>32,33</sup> A study by Ferreri and colleagues demonstrated  $K^{trans}$  as a useful biomarker to measure changes in BBB permeability of the vasculature and perilesional area in lymphoma before and after the injection of a permeabilizing agent.<sup>32</sup> Among all DCE-MRI parameters,  $K^{trans}$  is most consistently demonstrated its value in distinguishing differential diagnoses. The finding of higher values of  $K^{trans}$  in lymphoma when compared to other brain lesions like glioblastoma and metastases has been confirmed in several independent studies, and is consistent with the findings of other imaging modalities that are able to assess vascular permeability, like CT (computed tomography) perfusion and DSC-MRI.<sup>34,35</sup> In addition to  $K^{trans}$ , the extracellular volume fraction, termed " $V_e$ ," may differentiate lymphomas from other brain tumors; however, the true physiological interpretation is still debated.<sup>34</sup>  $V_e$  is defined as the volume of the extravascular extracellular space<sup>35</sup> and is thought to correlate with tumor cellularity.  $V_e$  is consistently been found to be higher in lymphoma than in glioblastoma and brain metastases, suggesting that this parameter may provide unique information about the tumor microenvironment and not specifically tumor cellularity.<sup>36</sup>

**Positron emission tomography.**—Positron emission tomography (PET) imaging with the radiolabeled glucose analog [<sup>18</sup>F]FDG has become the standard study for assessment of disease burden and management of systemic non-Hodgkin lymphoma.<sup>37</sup> While [<sup>18</sup>F]FDG is the dominant

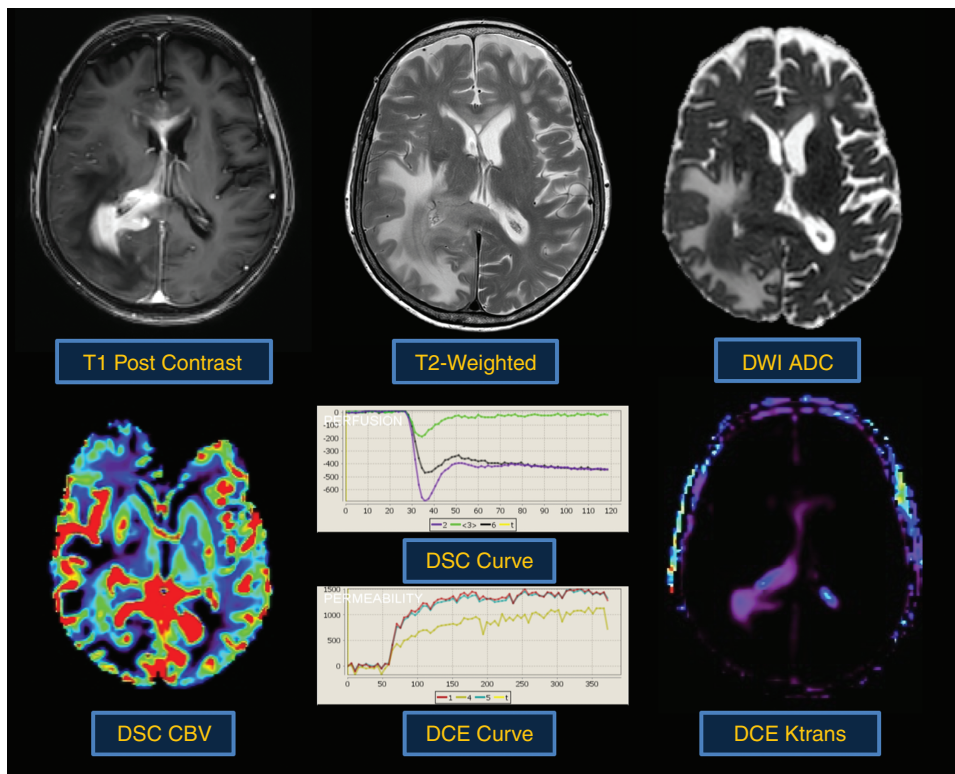


**Fig. 3** Typical morphologic and physiologic MRI appearance of PCNSL. PCNSL classically appears as a diffuse often periventricular enhancing mass (top left). T2-weighted imaging is often heterogenous but frequently demonstrates a mass like hypointense component (top middle) within enhancing regions. Increasing tumor cellularity is associated with decreasing T2 and ADC hypointensity (top right). Likewise, the degree of angiogenesis is reflected by DSC and DCE perfusion MRI sequences. CBV (bottom left) and  $K^{trans}$  (bottom right) are quite heterogenous in PCNSL and may be reflective of tumor aggressiveness.

radiotracer for PET imaging of hematological malignancies, other radiotracers such as radiolabeled amino acids and the cellular proliferation marker [ $^{18}\text{F}$ ]FLT (3- $^{18}\text{F}$ -fluoro-3-deoxythymidine) have also been investigated, mainly to differentiate tumor tissue from inflammation, to predict and evaluate therapy response, but also to improve image quality in areas of high [ $^{18}\text{F}$ ]FDG uptake such as the CNS. FLT may predict treatment outcome and patient prognosis earlier than imaging with FDG. In the brain, the amino acid tracers and FLT show negligible background activity and may provide information on treatment response and patient prognosis.

**Body PET.** Patients with CNS lymphoma and active disease outside of the CNS most often require the addition of chemotherapy targeting the non-CNS disease (eg, R-CHOP) in addition to a MTX-based chemotherapy for the CNS disease. Staging procedures typically identify a site of systemic disease in approximately 4%-7% of patients<sup>3,38</sup> and other secondary malignancies. Mohile et al. investigated the utility of [ $^{18}\text{F}$ ]FDG-body-PET retrospectively in 49 presumed PCNSL patients as part of systemic staging and observed that [ $^{18}\text{F}$ ]FDG-PET may be more sensitive than CT chest/abdomen/pelvis in the detection of systemic, non-CNS lymphomatous lesions.<sup>39</sup> Malani et al. reported that [ $^{18}\text{F}$ ]FDG-PET could identify secondary malignancies with

a sensitivity of 100% and a specificity of 86%, whereas CT chest/abdomen/pelvis had a sensitivity of 70% and a specificity of 77% in a retrospective review including 262 patients with newly diagnosed CNS lymphoma.<sup>38</sup> A higher standardized uptake value (SUV, a semiquantitative measure of glucose utilization) was associated with a higher risk of identifying a malignant lesion.

**Brain PET.** There are limited data on the value of brain PET in PCNSL and quantitative PET imaging biomarkers for PCNSL have not yet been established. [ $^{18}\text{F}$ ]FDG-PET may play a role in the diagnosis of PCNSL as brain PET may be able to differentiate PCNSL from other malignant brain tumors such as glioblastoma and metastasis,<sup>40</sup> since the majority of PCNSL lesions are highly FDG avid, with homogeneous uptake. Secondary to edema or disruption of tracts regulating cortical activity, overlying cortical gray matter can show glucose hypometabolism even when the lesion is located in the deep white matter, basal ganglia, or thalamus, further increasing lesion conspicuity. In a prospective study of 46 patients who underwent single-agent ibrutinib therapy and 15 receiving an ibrutinib/MTX combination therapy, a total of 85 lesions were identified. [ $^{18}\text{F}$ ]PET imaging parameters were measured and correlated with PFS.<sup>41</sup> High  $\text{SUV}_{\text{max}}$  was correlated with lower PFS. In patients with a  $\text{SUV}_{\text{max}} > 20$ , median PFS was

3.4 months, whereas patients with a  $SUV_{max} < 20$  had a median PFS of 10.8 months. Of note, several factors such as use of steroids, sedation, and the time between injection of radiotracer and imaging, may alter the degrees of [ $^{18}F$ ]FDG uptake in the brain and/or tumor.<sup>42</sup>

## Methods

### IPCG International Imaging Survey Rationale and Overview

The IPCG has recognized the need to develop updated consensus recommendations based, not only on recent advances in clinical research but also on modern clinical imaging practices across international sites. A push for consensus is provided in the context of an increasing realization that the rigor of clinical trials assessing response assessment can be improved by the reporting of imaging methodology and application of standardized imaging methods across institutions. The development of an updated standardized consensus protocol for conventional MRI in PCNSL can collaboratively build upon recently published recommendations in both glioma and metastases, which outline the minimal standard imaging requirements for conventional MRI.<sup>4,5</sup> At the same time, mounting evidence also supports the potential value of developing consensus recommendations for advanced physiologic imaging. The above discussion of advanced imaging techniques, such as DSC-MRI, DCE-MRI, DWI, and PET, underscores the promise of clinical applications in prognostication, prediction, diagnosis, and response assessment for PCNSL patients. A consensus protocol that includes advanced imaging will promote consistency across national and international clinical sites, and may expand the array of image-based predictive endpoints and biomarkers for future correlative studies and multicenter clinical trials.

To address these challenges, the IPCG imaging subcommittee surveyed members to determine the common (conventional and advanced physiologic) clinical imaging practices for the evaluation of PCNSL at institutions across the world. The questions focused particularly on the following: (1) common practice and technical capabilities for performing volumetric imaging; (2) interest in adoption of advanced physiologic MRI techniques for PCNSL assessment; and (3) common practice for PET imaging in the evaluation of PCNSL

## Results

### IPCG Survey Results

**Response demographics.**—The survey was electronically distributed to large international distributions lists (200+ emails) that represented 147 medical institutions, consisting of network members in the IPCG (N = 66), the UK National Cancer Research Institute (NCRI) PCNSL working group (N = 16), and the distribution lists for sites participating in the International Extranodal Lymphoma Study Group IELSG20 (N = 25) and IELSG32 (N = 40)

clinical trials. From these distribution lists, 33 responses were received from 29 different institutions (from 9 countries; [Figure 4](#); [Supplementary online data](#)).

### Equipment and field strength used for MRI of PCNSL.

—The majority of institutions acquire MRI scans on either 1.5T or 3T (63.65%), compared to 3T only (24.25%) or 1.5T only (9.1%). Most sites use a 16-40 channel head or head/neck coil (64.5%), compared to 64-128 channel head or head/neck coil (16.1%) or 4-8 channel head coil (6.4%).

### Conventional MRI sequence types.

—For T2/FLAIR imaging, most sites use 2D FLAIR (62.5%), while the rest of the sites acquired both 2D and 3D volumetric acquisitions (20.8%) or 3D volumetric alone (16.7%). For T1W pre-contrast imaging, most use 2D acquisition (53.8%), compared to 3D volumetric (38.5%) or both 2D and 3D acquisitions (7.7%). For T1W post-contrast imaging, most use 3D volumetric (48.1%) or both 2D and 3D acquisitions (29.6%), while only (22.2%) use only 2D acquisitions.

### Advanced physiologic MRI sequences.

—For DWI, most used DWI (90.3%), while 6.5% used both diffusion tensor imaging (DTI) and DWI. Only one site (3.2%) did not employ DWI or DTI. For DSC-MRI perfusion, 35.5% of sites employed DSC in the evaluation of PCNSL. For most that did not perform DSC routinely, common reasons for not doing so included: lack of validated data for clinical utility in PCNSL, perceived time limitations, or they perform DCE-MRI exclusively. However, 85.7% of sites were agreeable to performing DSC as part of the clinical trial assessment of PCNSL to help establish the clinical utility of the technique. Of those sites using DSC-MRI, 88.9% use GE vs 11.1% use SE. A third of sites (33.3%) use preload dose (PLD) to minimize T1W leakage effects. For DCE-MRI perfusion, 27.6% of sites employed DCE for the assessment of PCNSL. For PET imaging, 17.9% of sites performed PET imaging routinely at baseline for assessment of PCNSL, but not routinely on follow-up. Another 53.55% of sites reported only periodically using PET on a case-by-case basis. 28.55% of sites report never using PET. Of the sites that perform PET, all (100%) use FDG as the PET radiotracer. The majority of sites (66.7%) use whole body PET imaging in suspected PCNSL to rule out systemic disease.

## Discussion

### IPCG Consensus Recommendations for MRI and PET Imaging Protocols

**Conventional contrast-enhanced MRI and the “minimal standard” recommended pulse sequences.**—Recent consensus recommendations have proposed “minimal standard” imaging protocols for both glioma and brain metastases.<sup>4,5</sup> These recommendations have reviewed the advantages of high-resolution 3D volumetric acquisitions, as well as SE (vs GE)-based acquisitions for T1W post-contrast sequences. The IPCG recommendations for

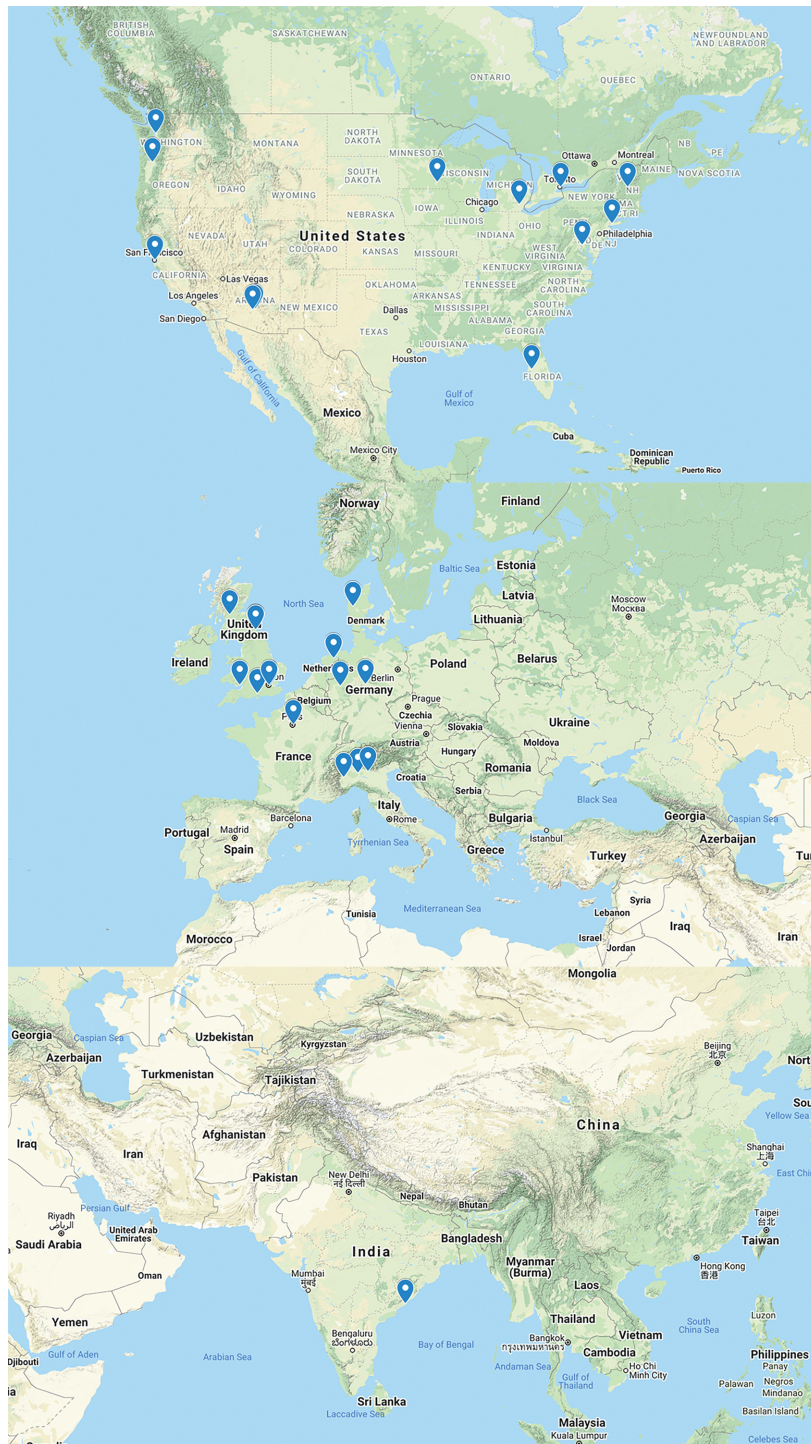


**Fig. 4** Demographic distribution of IPCG survey response. The IPCG imaging subcommittee surveyed members to determine clinical imaging practices for the evaluation of PCNSL at institutions across the world. About 147 institutions were invited to participate in this electronic survey. A 20% response rate was received from institutions delineated on the map from North America (N = 11), Europe (N = 17), and India (N = 1). Abbreviations: IPCG, International PCNSL Collaborative Group; PCNSL, primary central nervous system lymphoma.

PCNSL imaging, presented here, build collaboratively up on recent imaging consensus recommendations, as listed in [Tables 1–3](#). These recommendations include adherence to specified standards for image resolution.<sup>4,5</sup>

For example, we recommend that 3D anatomic images are acquired at 1-1.5 mm isotropic voxel size, and 2D anatomic images are acquired at <4 mm contiguous slices. The IPCG recognizes that clinical sites have varying degrees



of MRI scanner performance and sequence capabilities. With this in mind, separate protocols have been listed for ideal (Table 1) and minimal standard (Table 2) conditions at 3T field strength, as well as at 1.5T field strength (Table 3). In short, the ideal MRI protocol will be performed at 3T field strength utilizing SE volumetric T1W (pre- and post-contrast-enhanced), T2W, and CE-T2W-FLAIR sequences with 1 mm isotropic resolution (Table 1). Fast or turbo spin-echo (FSE/TSE) T1-weighted sequences allows for an adaptation of the conventional SE acquisition technique while providing for reduced image acquisition time. FSE/TSE is preferred to inversion-recovery gradient echo (IR-GRE) sequence for the acquisition of pre- and post-contrast T1-weighted imaging. FSE/TSE provides for improved signal-to-noise (SNR) ratios for the detection of T1 signal. If volumetric TSET1-weighted imaging cannot be performed, we recommend that a 2D thin slice (no interslice gap with less than 4 mm slices) SE (SE or FSE/TSE) sequence be performed prior to IR-GRE post-gad T1 imaging. This additional SE sequence may allow for the detection of small or subtle enhancing foci that are not expected to be appreciated by IR-GRE sequences. Whenever possible, pre- and post-gadolinium sequences should be congruent. The use of gadolinium contrast agents at a standard clinical dose of 0.1 mmol/kg is recommended for initial and follow-up PCNSL imaging time points. The standardization of post-gadolinium imaging sequences is also desired. T1-weighted imaging should be initiated in the 4- to 8-min time frame following intravenous contrast administration. This can be facilitated by performing both DSC perfusion and FLAIR imaging sequentially prior to post-contrast T1-weighted imaging. The use of both TSET2-weighted and CE-T2W-FLAIR sequences is recommended.

The IPCG recommends CE-T2W-FLAIR sequence acquisition, instead of T2-weighted sequence, be performed as the immediate sequence following intravenous gadolinium contrast administration (Tables 1–3). It is proposed that the use of CE-T2W-FLAIR will provide for improved sensitivity for the detection of T1 and T2 hyperintense foci. The clinical utility of this technique may be most helpful in the evaluation of subtle lepto- and pachymeningeal disease.<sup>43</sup> The consideration for non-tumoral etiologies of CE-FLAIR leptomeningeal signal should be considered, despite their low probability in the context of PCNSL. When possible, the same scanner capabilities (identical field strength and imaging protocol) should be utilized for follow-up imaging.

**Diffusion.**—DWI is established as standard of care for almost all diagnostic brain imaging. Various techniques with increasing complexity have been described for DWI. IPCG imaging recommendations focus on obtaining the most widely available DWI technique that allows for the generation of ADC maps. Our minimum recommendation for DWI sequence acquisition includes the use of three *b* values of 0, 500, and 1000 s/mm<sup>2</sup>.<sup>44</sup> Likewise, a minimum of three orthogonal diffusion directions should be obtained. However, more advanced DWI techniques using multiple *b* values and multiple diffusion directions (eg, DTI) may be considered, but should include the recommendations which allow for the generation of consistent ADC values and comparisons across clinical trials. As detailed in Tables 1–3, IPCG

recommends the use of 2D 3 mm slice thickness single-shot echo-planar imaging (SS-EPI) sequence for the fast acquisition of DWI. The use of radial readout-segmented echo-planar diffusion methods is discouraged except in the case of extreme uncorrectable patient motion.

**DSC perfusion.**—There has been progress in developing consensus recommendations for DSC-MRI methodology.<sup>6,45,46</sup> Single-echo GRE echo-planar imaging is generally accepted to provide more robust rCBV measurements of tumoral microvasculature compared to SE for brain tumors. GRE CBV maps have higher inherent SNR and sensitivity than SE CBV maps, and can provide greater signal changes for equal GBCA dose, or equivalent signal changes with lower gadolinium based contrast agent (GBCA) dose, as compared to SE DSC-MRI.<sup>47</sup>

The most accepted methods to minimize T1W leakage effects of extravascular GBCA are: (1) use of a preload contrast dose (PLD)<sup>48</sup>; (2) low flip angle (FA)<sup>28,48,49</sup>; and (3) post-processing model-based leakage correction.<sup>48,50</sup> The current gold-standard DSC-MRI protocol is the use of a single-dose PLD (ie, 0.1 mmol/kg) followed by a second single-dose bolus injection (0.1 mmol/kg) for the DSC-MRI acquisition (eg, “1 + 1” dosing scheme) using a moderate FA (eg, 60°).<sup>47–51</sup> The “1 + 1” moderate FA protocol has shown strong correlation with histologic distinction between tumor and non-tumoral posttreatment-related effects (eg, pseudoprogression, radiation necrosis), as well as strong correlation with microvascular volume tissue benchmarks.

Given the requirement for double-dose GBCA for the “1 + 1” dosing scheme and growing concern for gadolinium deposition in the brain or body, many sites elect to keep total GBCA contrast administration to a single total dose (ie, 0.1 mmol/kg). The most common method is to omit the PLD and administer only a single dose for the DSC-MRI bolus acquisition (ie, “0 + 1” dosing scheme). This dosing paradigm is compatible with the BTIP, which mandates that post-contrast T1W imaging be performed after a single total dose of GBCA. Simulation studies<sup>6,45</sup> suggest that if single-dose options are used (eg, “0 + 1,” “ $\frac{1}{4}$  +  $\frac{3}{4}$ ,” “ $\frac{1}{2}$  +  $\frac{1}{2}$ ”), then the use of a low FA with an optimized echo time (30° and 30 ms @ 3T) provides significantly higher rCBV accuracy, when model-based leakage correction strategies (eg, Boxerman-Schminda-Weisskoff (BSW) model, bidirectional).<sup>6,45,52</sup> Preliminary studies suggest comparable rCBV measurements when comparing the low FA “0 + 1” protocol with the benchmark standard (moderate FA “1 + 1” protocol).<sup>6,51</sup> While further studies are underway, these initial results form the basis of the IPCG recommendations to utilize a low FA protocol (eg, 30°) with single-dose administration (eg, 0 + 1) being preferred rather than the less ideal fractional dosing protocols (“ $\frac{1}{4}$  +  $\frac{3}{4}$ ,” “ $\frac{1}{2}$  +  $\frac{1}{2}$ ”). Post-processing leakage correction (eg, BSW, bidirectional) should be used for all cases, regardless of the PLD protocol employed.

**Whole body FDG-PET.**—To identify systemic, non-CNS lymphoma in patients with lymphomatous brain lesions, the IPCG recommends a systemic staging evaluation, including CT of the chest, abdomen, and pelvis, PET of the torso (from mid skull to upper thigh), and bone marrow

**Table 1** “Ideal” Recommended PCNSL 3T MRI Protocol\*

	DWI	T1W-Pre <sup>b</sup>	T2W	Contrast Injection <sup>a</sup>		
				DSC Perfusion <sup>a, #, ^</sup>	CE-T2W-FLAIR	T1W-Post <sup>b, e</sup>
Sequence	SS-EPI <sup>d</sup>	TSE <sup>c, f</sup>	TSE <sup>c</sup>	GE-EPI	TSE <sup>c</sup>	TSE <sup>f</sup>
Plane	Axial	Any	Any	Axial	Any	Any
Mode	2D	3D	3D	2D	3D <sup>i</sup>	3D
TR (ms)	>5000	550-750	>2500	1000-1500	>6000	550-750
TE (ms)	Min	Min	80-120	20-35 ms	90-140	Min
TI (ms)					2000-2500	
Flip angle	90°/180°	Default <sup>g</sup>	90°/≥160°	30-35°	90°/≥160°	Default <sup>g</sup>
Frequency	128	256	≥256	≥96	≥256	256
Phase	128	256	≥256	≥96	≥256	256
NEX	≥1	≥1	≥1	1	≥1	≥1
FOV	240 mm	256 mm	240 mm	240 mm	240 mm	256 mm
Slice thickness	3 mm	1 mm	1 mm	3-5 mm as needed to cover tumor	1 mm	1 mm
Spacing	0	0	0	0-1 mm as needed to cover tumor	0	0
Other options	$b = 0, 500$ and $1000$ s/mm <sup>2</sup> , ≥3 directions	Consider fat saturation		30-60 pre-bolus time points; >120 total time points; centered on tumor. DCE is optional before DSC	Consider fat saturation	Consider fat saturation
Parallel imaging <sup>h</sup>	Up to 2x	Up to 2x	Up to 2x	Up to 2x	Up to 2x	Up to 2x
Estimated time (min) <sup>j</sup>	2-4	5-8	5-8	2-4	5-8	5-8

**Abbreviations:** CE-T2W-FLAIR, contrast-enhanced T2-weighted fluid-attenuated inversion recovery; DSC, dynamic susceptibility contrast; DWI, diffusion-weighted imaging; GE-EPI, gradient echo echo-planar imaging; PCNSL, primary central nervous system lymphoma; SS-EPI, single-shot echo-planar imaging; TSE, turbo spin echo.

<sup>a</sup>0.1 mmol/kg dose injection with a gadolinium-chelated contrast agent as a single total dose is recommended. For DSC perfusion, contrast injection is performed after obtaining 30-50 DSC time points. In the absence of performing DCE, no DSC preload contrast dose is recommended given use of low flip angle. DSC perfusion can be performed with the “ideal” protocol at 3T as well as with the “minimum standard” protocols at 3T and 1.5T. The use of a power injector is desirable at an injection rate of 3-5 cc/sec.

<sup>#</sup>If both DCE and DSC acquisitions are desired and performed on 3T unit, the 0.1 mmol/kg (single total dose) can be split into 2 separate half doses (½ + ½) over two sequential injections. Alternatively, for clinical sites that employ a double-dosing protocol, a 0.2 mmol/kg (double total dose) can be split into 2 separate single doses (1 + 1) over two sequential injections. For both dosing protocols, DCE will be acquired during the first injection, and DSC will be acquired during the second injection. However, for the (1 + 1) dose schema, the post-contrast T1-weighted image should be acquired after DCE and before DSC, per the standardized DSC recommendations for high-grade gliomas.<sup>6</sup>

<sup>^</sup>If only DCE acquisition is desired, the DCE sequence will replace the DSC and employ the full single dose (0.1 mmol/kg) contrast injection.

<sup>b</sup>Post-contrast 3D T1-weighted images should be collected with equivalent parameters to pre-contrast 3D T1-weighted images.

<sup>c</sup>TSE = turbo spin echo (Siemens and Philips) is equivalent to FSE (fast spin echo); GE, Hitachi, Toshiba).

<sup>d</sup>In the event of significant patient motion, a radial acquisition scheme may be used (eg, BLADE [Siemens], PROPELLER [GE], MultiVane [Philips], RADAR [Hitachi], or JET [Toshiba]); however, this acquisition scheme can cause significant differences in ADC quantification and should be used only if EPI is not an option. Furthermore, this type of acquisition takes considerable more time.

<sup>e</sup>3D post-contrast T1-weighted images are collected between 4 and 8 min after contrast injection and this timing is constant across all MR exams performed in each patient.

<sup>f</sup>Acceptable 3D T1W TSE sequences include CUBE (GE), SPACE (Siemens), VISTA (Philips), isoFSE (Hitachi), or 3D MVOX (Canon).

<sup>g</sup>Flip angles for 3D TSE sequences (including CUBE and SPACE) are complicated because many utilize variable flip angle refocusing radiofrequency pulses to produce the desired image contrast. Investigators are encouraged to work with their scanner vendors to determine the ideal parameters.

<sup>h</sup>Investigators are encouraged to work with their scanner vendors to determine the best parallel imaging strategies, which may include simultaneous multislice imaging (SMS), controlled aliasing in parallel imaging resulting in higher acceleration (CAIPI), iPAT, GRAPPA, as well as turbo or other acceleration factors. High performance MRI scanners may be capable of higher acceleration factors.

<sup>i</sup>2D FLAIR is an optional alternative to 3D FLAIR, with sequence parameters as follows per previously published recommendations (Kaufmann et al): 2D TSE/FSE acquisition; TE = 100-140 ms; TR = >6000 ms; TI = 2000-2500 ms (chosen based on vendor recommendations for optimized protocol and field strength); GRAPPA ≤ 2; fat suppression; slice thickness ≤ 3 mm; orientation axial; FOV ≤ 250 mm × 250 mm; matrix ≥ 244 × 244.

<sup>j</sup>Imaging times provided as an estimation only. Exact imaging times will depend upon individual scanner and hardware performance capabilities.

\*Adapted from Refs.<sup>4-6</sup>

biopsy. Patient preparation and image acquisition need to be standardized. Critically for [<sup>18</sup>F]FDG-PET, patients need to fast for 4-6 h prior to the IV injection of the radiotracer

(to reduce competition of radiolabeled deoxyglucose with plasma glucose). Blood glucose levels should be below 200 mg/dl. In general, patients are injected with 8-12 mCi

**Table 2** “Minimum” Recommended PCNSL 3T MRI Protocol\*

	DWI	T1W-Pre <sup>b</sup>	T2W	Contrast Injection <sup>a</sup>			
				DSC Perfusion <sup>a, #, ^</sup>	CE-T2W-FLAIR	T1W-Post <sup>a, q</sup>	T1W-Post <sup>b, e</sup>
Sequence	SS-EPI <sup>d</sup>	IR-GRE <sup>f, i, j, k</sup>	TSE <sup>c</sup>	GE-EPI	TSE <sup>c</sup>	TSE/SE	IR-GRE <sup>f, i, k</sup>
Plane	Axial	Any	Any	Axial	Any	Axial	Any
Mode	2D	3D	3D <sup>n</sup>	2D	3D <sup>n, i</sup>	2D	3D
TR (ms)	>5000	2100 <sup>l</sup>	>2500	1000-1500	>6000	400-600	2100 <sup>l</sup>
TE (ms)	Min	Min	80-120	20-35 ms	90-140	Min	Min
TI (ms)		1100 <sup>m</sup>			2000-2500		1100 <sup>m</sup>
Flip angle	90°/180°	10°-15°	90°/≥160°	30-35°	90°/≥160°	90°/≥160°	10°-15°
Frequency	128	256	≥256	≥96	≥256	256	256
Phase	128	256	≥256	≥96	≥256	256	256
NEX	≥1	≥1	≥1	1	≥1	≥1	≥1
FOV	240 mm	256 mm	240 mm	240 mm	240 mm	240 mm	256 mm
Slice thickness	3 mm	1 mm	1 mm	3-5 mm as needed to cover tumor	1 mm	3 mm	1 mm
Spacing	0	0	0	0-1 mm as needed to cover tumor	0	0	0
Other options	$b = 0, 500$ and $1000$ s/mm <sup>2</sup> , ≥3 directions	Consider fat saturation		30-60 pre-bolus time points; >120 total time points; centered on tumor. DCE is optional before DSC	Consider fat saturation	Consider fat saturation	Consider fat saturation
Parallel imaging <sup>h</sup>	Up to 2x	Up to 2x	Up to 2x	Up to 2x	Up to 2x	Up to 2x	Up to 2x
Estimated time (min) <sup>p</sup>	2-4	5-8	5-8	2-4	5-8	3-5	5-8

**Abbreviations:** CE-T2W-FLAIR, contrast-enhanced T2-weighted fluid-attenuated inversion recovery; DCE, dynamic contrast-enhanced; DSC, dynamic susceptibility contrast; DWI, diffusion-weighted imaging; GE-EPI, gradient echo echo-planar imaging; IR-GRE, inversion recovery gradient echo; PCNSL, primary central nervous system lymphoma; SE, spin echo; SS-EPI, single-shot echo-planar imaging; TSE, turbo spin echo.

<sup>a</sup>0.1 mmol/kg dose injection with a gadolinium-chelated contrast agent as a single total dose is recommended. For DSC perfusion, contrast injection is performed after obtaining 30-50 DSC time points. In the absence of performing DCE, no DSC pre-load contrast dose is recommended given use of low flip angle. DSC perfusion can be performed with the “ideal” protocol at 3T as well as with the “minimum standard” protocols at 3T and 1.5T. The use of a power injector is desirable at an injection rate of 3-5 cc/sec.

<sup>#</sup>If both DCE and DSC acquisitions are desired and performed on 3T unit, the 0.1 mmol/kg (single total dose) can be split into 2 separate half doses ( $\frac{1}{2} + \frac{1}{2}$ ) over two sequential injections. Alternatively, for clinical sites that employ a double-dosing protocol, a 0.2 mmol/kg (double total dose) can be split into 2 separate single doses (1 + 1) over two sequential injections. For both dosing protocols, DCE will be acquired during the first injection, and DSC will be acquired during the second injection. However, for the (1 + 1) dose schema, the post-contrast T1-weighted image should be acquired after DCE and before DSC, per the standardized DSC recommendations for high-grade gliomas.<sup>31</sup>

<sup>^</sup>If only DCE acquisition is desired, the DCE sequence will replace the DSC and employ the full single dose (0.1 mmol/kg) contrast injection.

<sup>b</sup>Post-contrast 3D T1-weighted images should be collected with equivalent parameters to pre-contrast 3D T1-weighted images.

<sup>c</sup>TSE = turbo spin echo (Siemens and Philips) is equivalent to FSE (fast spin echo; GE, Hitachi, Toshiba).

<sup>d</sup>In the event of significant patient motion, a radial acquisition scheme may be used (eg, BLADE [Siemens], PROPELLER [GE], MultiVane [Philips], RADAR [Hitachi], or JET [Toshiba]); however, this acquisition scheme can cause significant differences in ADC quantification and should be used only if EPI is not an option. Furthermore, this type of acquisition takes considerable more time.

<sup>e</sup>3D post-contrast T1-weighted images are collected between 4 and 8 min after contrast injection and this timing is constant across all MR exams performed in each patient.

<sup>f</sup>Acceptable 3D T1W TSE sequences include CUBE (GE), SPACE (Siemens), VISTA (Philips), isoFSE (Hitachi), or 3D MVOX (Canon).

<sup>h</sup>Investigators are encouraged to work with their scanner vendors to determine the best parallel imaging strategies, which may include simultaneous multislice imaging (SMS), controlled aliasing in parallel imaging resulting in higher acceleration (CAIPI), iPAT, GRAPPA, as well as turbo or other acceleration factors. High performance MRI scanners may be capable of higher acceleration factors.

<sup>i</sup>2D FLAIR is an optional alternative to 3D FLAIR, with sequence parameters as follows per previously published recommendations (Kaufmann et al.): 2D TSE/FSE acquisition; TE = 100-140 ms; TR = >6000 ms; TI = 2000-2500 ms (chosen based on vendor recommendations for optimized protocol and field strength); GRAPPA ≤ 2; fat suppression; slice thickness ≤ 3 mm; orientation axial; FOV ≤ 250 mm × 250 mm; matrix ≥ 244 × 244. FL2D = two-dimensional fast low angle shot (FLASH; Siemens) is equivalent to the spoiled gradient-recalled echo (SPGR; GE) or T1-fast field echo (FFE; Philips), fast field echo (FastFE; Toshiba), or the radiofrequency spoiled steady-state acquisition rewound gradient echo (RSSG; Hitachi). A fast gradient echo sequence without inversion preparation is desired.

**Table 2** Continued

<sup>j</sup>IR-GRE = inversion-recovery gradient-recalled echo sequence is equivalent to MPRAGE = magnetization prepared rapid gradient-echo (Siemens and Hitachi) and the inversion-recovery spoiled gradient-echo (IR-SPGR or Fast SPGR with inversion activated or BRAVO; GE), 3D turbo field echo (TFE; Philips), or 3D fast field echo (3D Fast FE; Toshiba).

<sup>k</sup>A 3D acquisition without inversion preparation will result in different contrast compared with MPRAGE or another IR-prepped 3D T1-weighted sequences and therefore should be avoided.

<sup>l</sup>For Siemens and Hitachi scanners. GE, Philips, and Toshiba scanners should use a TR = 5-15 ms for similar contrast.

<sup>m</sup>For Siemens and Hitachi scanners. GE, Philips, and Toshiba scanners should use a T1 = 400-450 ms for similar contrast.

<sup>n</sup>2D TSE should be performed if 3D volumetric sequence is not available. Minimal slice thickness should be utilized for 2D sequence.

<sup>o</sup>If IR-GRE T1W imaging is utilized in place of 3D TSE then 2D post-contrast TSE/SE sequence is recommended prior to IR-GRE T1W.

<sup>p</sup>Imaging times provided as an estimation only. Exact imaging times will depend upon individual scanner and hardware performance capabilities.

<sup>q</sup>Patient comfort and potential for movement may require 3D T1W IR-GRE sequence prior to the 2D T1W TSE/SE. However, diminished lesion conspicuity observed with 3D T1W IR-GRE sequence can be improved by delaying acquisition until the end of the examination.

\*Adapted from Refs.<sup>4-6</sup>

(296-444 MBq) FDG for body imaging, lower activities can be utilized for brain-only imaging. After injection, patients should rest in a quiet room for 60-90 min before the image acquisition.

Body scans are generally acquired from the mid skull to the upper thigh. Abnormal [<sup>18</sup>F]-FDG uptake (a "lesion") is generally defined as non-physiologic uptake with intensity greater than background activity and without benign correlates (such as pneumonia or a fracture) on the corresponding CT. PET metrics include the SUV (reflecting the intensity of uptake), metabolic tumor volume (MTV; the volume of FDG-avid disease), and total lesion glycolysis (TLG; the product of mean SUV and MTV). Acquisition and interpretation criteria for other radiotracers, such as various amino acids, are currently being defined.

### Optional Imaging Sequences

**DCE perfusion.**—While DSC represents the most commonly employed technique to assess tissue/tumoral perfusion in the brain, it remains an optional sequence for patients with PCNSL. The most common method for estimating baseline T1 is through the use of a series of fast 3D GE sequences (eg, spoiled gradient-recalled echo [SPGR] or fast low angle shot [FLASH]) with different FAs, often 2-7 different FAs ranging from 2° to 30°, repetition time (TR) = 3-7 ms, minimal echo time (TE) (typically between 1 and 2.5 ms), slice thickness 5 mm or less, no interslice gap, and an acquisition matrix of 25 × 128-160. After T1 mapping, the same base sequence, TE, TR, and spatial resolution and a fixed FA of between 25° and 35° is employed for the dynamic acquisition of DCE data, ensuring a temporal resolution of less than 10 s. A minimum of 5 phases should be acquired before contrast agent injection to adequately sample the baseline signal intensity. 40-80 phases is sufficient for at least 5-6 min of post-IV gadolinium injection imaging acquisition. The IV contrast injection rate may be 3-5 ml/sec. For data analysis, Quantitative Imaging Biomarkers Alliance® (QIBA) recommends the use of a DCE-MRI tool that computes the pharmacokinetic parameters ( $K^{\text{trans}}$  and  $V_e$ ) using the standard Tofts' model.<sup>35</sup>

**Brain PET.**—While the use of [<sup>18</sup>F]FDG-body PET for staging purposes and identification of systemic disease has been established and can be pivotal in the patient's treatment decisions, the role of a dedicated FDG brain PET scan is less clear. At this time, the IPCG deems the acquisition of brain FDG-PET as optional for patients with PCNSL. If this study is obtained it is important that brain cortical stimulation during the uptake time must be avoided and dedicated brain scans are acquired for 10-15 min. FDG shows high physiologic uptake (reflecting high glucose metabolism) in the cortex, thalami, basal ganglia. Nevertheless, since many malignant tumors present initially within the white matter (which has no or only minimal FDG uptake), higher grade and aggressive tumors, including CNS lymphomas, are usually well recognized and characterized.

### Implications of Implementing PCNSL Imaging Protocol

The design and implementation of robust clinical trials are necessarily time, labor, and cost-intensive. The lack of standardized imaging protocols can introduce unintended errors and degrade the scientific rigor of correlative outcome analyses in multi-institutional studies. To this end, the IPCG seeks to reduce imaging variability through the development of standardized consensus recommendations, with the overarching goal of developing more consistent and reliable surrogate measures of clinical trial outcomes.

The IPCG consensus recommendations are aimed to maximize the clinical utility of imaging data while remaining within clinically feasible scan times (ie, 45 min or less) and technical capabilities for both community- and academic-based institutions. These recommendations utilize the minimal number of sequences to ensure therapeutic assessment is achievable and provides options when patient motion is a complicating factor. This standardized imaging approach is also expected to be important for optimizing response assessment in frail symptomatic patients for whom prolonged examinations are untenable. With these recommendations, the IPCG provides an "ideal"

**Table 3** “Minimum” Recommended PCNSL 1.5T MRI Protocol<sup>a</sup>

	DWI	T1W-Pre <sup>b</sup>	T2W	Contrast Injection <sup>a</sup>			
				DSC Perfusion <sup>a,^</sup>	CE-T2W-FLAIR	T1W-Post <sup>o,s</sup>	T1W-Post <sup>b,e</sup>
Sequence	SS-EPI <sup>d</sup>	IR-GRE <sup>f,i,j,k</sup>	TSE <sup>c</sup>	GE-EPI	TSE <sup>c</sup>	TSE/SE	IR-GRE <sup>f,i,j,k</sup>
Plane	Axial	Any	Any	Axial	Any	Axial	Any
Mode	2D	3D	3D <sup>n</sup>	2D	3D <sup>n,i</sup>	2D <sup>p</sup>	3D
TR (ms)	>5000	2100 <sup>l</sup>	>2500	1000-1500	>6000	400-600	2100 <sup>l</sup>
TE (ms)	Min	Min	80-120	45 ms	90-140	Min	Min
TI (ms)		1100 <sup>m</sup>			2000-2500		1100 <sup>m</sup>
Flip angle	90°/180°	10°-15°	90°/≥160°	30-35°	90°/≥160°	90°/≥160°	10°-15°
Frequency	128	172	≥256	≥96	≥256	≥256	≥172
Phase	128	172	≥256	≥96	≥256	≥256	≥172
NEX	≥1	≥1	≥1	1	≥1	≥1	≥1
FOV	240 mm	256 mm	240 mm	240 mm	240 mm	240 mm	256 mm
Slice thickness	≤4 mm	≤1.5 mm	≤1.5 mm	3-5 mm as needed to cover tumor <sup>q</sup>	≤1.5 mm	≤4 mm	≤1.5 mm
Spacing	0	0	0	0-1 mm as needed to cover tumor	0	0	0
Other options	<i>b</i> = 0, 500 and 1000 s/mm <sup>2</sup> ≥3 directions	Consider fat saturation		30-60 pre-bolus time points; >120 total time points; centered on tumor. Either DCE or DSC is recommended at 1.5T	Consider fat saturation	Consider fat saturation	Consider fat saturation
Parallel imaging <sup>h</sup>	Up to 2x	Up to 2x	Up to 2x	Up to 2x	Up to 2x	Up to 2x	Up to 2x
Estimated time (min) <sup>r</sup>	2-5	5-10	5-10	2-4	5-10	3-6	5-10

**Abbreviations:** CE-T2W-FLAIR, contrast-enhanced T2-weighted fluid-attenuated inversion recovery; DCE, dynamic contrast-enhanced; DSC, dynamic susceptibility contrast; DWI, diffusion-weighted imaging; GE-EPI, gradient echo echo-planar imaging; IR-GRE, inversion recovery gradient echo; PCNSL, primary central nervous system lymphoma; SE, spin echo; SS-EPI, single-shot echo-planar imaging; TSE, turbo spin echo.

<sup>a</sup>0.1 mmol/kg dose injection with a gadolinium-chelated contrast agent as a single total dose is recommended. For DSC perfusion, contrast injection is performed after obtaining 30-50 DSC time points. In the absence of performing DCE, no DSC preload contrast dose is recommended given use of low flip angle. DSC perfusion can be performed with the “ideal” protocol at 3T as well as with the “minimum standard” protocols at 3T and 1.5T. The use of a power injector is desirable at an injection rate of 3-5 cc/sec.

<sup>^</sup>At 1.5T only DCE or DSC is recommended. If only DCE acquisition is desired, the DCE sequence will replace the DSC and employ the full single dose (0.1 mmol/kg) contrast injection. Given the limitations of contrast-to-noise ratio at 1.5T field strength, ½ + ½ dosing is not recommended. As such, the use of a total single dose (0.1 mmol/kg) cannot accommodate the acquisition of both DCE and DSC, unless larger contrast dosage is employed.

<sup>b</sup>Post-contrast 3D T1-weighted images should be collected with equivalent parameters to pre-contrast 3D T1-weighted images.

<sup>c</sup>TSE = turbo spin echo (Siemens and Philips) is equivalent to FSE (fast spin echo; GE, Hitachi, Toshiba).

<sup>d</sup>In the event of significant patient motion, a radial acquisition scheme may be used (eg, BLADE [Siemens], PROPELLER [GE], MultiVane [Philips], RADAR [Hitachi], or JET [Toshiba]); however, this acquisition scheme can cause significant differences in ADC quantification and should be used only if EPI is not an option. Furthermore, this type of acquisition takes considerable more time.

<sup>e</sup>3D post-contrast T1-weighted images are collected between 4 and 8 min after contrast injection and this timing is constant across all MR exams performed in each patient.

<sup>f</sup>Acceptable 3D T1W TSE sequences include CUBE (GE), SPACE (Siemens), VISTA (Philips), isoFSE (Hitachi), or 3D MVOX (Canon).

<sup>h</sup>Investigators are encouraged to work with their scanner vendors to determine the best parallel imaging strategies, which may include simultaneous multislice imaging (SMS), controlled aliasing in parallel imaging resulting in higher acceleration (CAIPI), iPAT, GRAPPA, as well as turbo or other acceleration factors. High performance MRI scanners may be capable of higher acceleration factors.

<sup>i</sup>2D FLAIR is an optional alternative to 3D FLAIR, with sequence parameters as follows per previously published recommendations (Kaufmann et al): 2D TSE/FSE acquisition; TE = 100-140 ms; TR = >6000 ms; TI = 2000-2500 ms (chosen based on vendor recommendations for optimized protocol and field strength); GRAPPA ≤ 2; fat suppression; slice thickness ≤ 3 mm; orientation axial; FOV ≤ 250 mm × 250 mm; matrix ≥ 244 × 244. FL2D = two-dimensional fast low angle shot (FLASH; Siemens) is equivalent to the spoiled gradient-recalled echo (SPGR; GE) or T1-fast field echo (FFE; Philips), fast field echo (FastFE; Toshiba), or the radiofrequency spoiled steady-state acquisition rewind gradient echo (RSSG; Hitachi). A fast gradient echo sequence without inversion preparation is desired.

<sup>l</sup>IR-GRE = inversion-recovery gradient-recalled echo sequence is equivalent to MPRAGE = magnetization prepared rapid gradient-echo (Siemens and Hitachi) and the inversion-recovery spoiled gradient-echo (IR-SPGR or Fast SPGR with inversion activated or BRAVO; GE), 3D turbo field echo (TFE; Philips), or 3D fast field echo (3D Fast FE; Toshiba).

<sup>k</sup>A 3D acquisition without inversion preparation will result in different contrast compared with MPRAGE or another IR-prepped 3D T1-weighted sequences and therefore should be avoided.

<sup>r</sup>For Siemens and Hitachi scanners. GE, Philips, and Toshiba scanners should use a TR = 5-15 ms for similar contrast.

**Table 3** Continued

- <sup>m</sup>For Siemens and Hitachi scanners. GE, Philips, and Toshiba scanners should use a TI = 400-450 ms for similar contrast.
- <sup>n</sup>2D TSE should be performed if 3D volumetric sequence is not available. Minimal slice thickness should be utilized for 2D sequence.
- <sup>o</sup>If IR-GRE T1W imaging is utilized in place of 3D TSE then 2D post-contrast TSE/SE sequence is recommended prior to IR-GRE T1W.
- <sup>p</sup>Whenever possible 3D TSE is recommended as the preferred T1W sequence. If 3D TSE is able to be performed at 1.5T, then IR-GRE sequences should be eliminated.
- <sup>q</sup>If the lesion extends beyond the original DSC coverage of tumor, an increase in slice thickness (up to 5 mm) or increase in gap could be considered to ensure adequate coverage.
- <sup>r</sup>Imaging times provided as an estimation only. Exact imaging times will depend upon individual scanner and hardware performance capabilities.
- <sup>s</sup>Patient comfort and potential for movement may require 3D T1W IR-GRE sequence prior to the 2D T1W TSE/SE. However, diminished lesion conspicuity observed with 3D T1W IR-GRE sequence can be improved by delaying acquisition until the end of the examination.
- \*Adapted from Refs.<sup>4-6</sup>

and “minimal” protocol to facilitate wide adaptability among institutions with variability in scanner performance and capabilities. The “ideal” MRI protocol is optimized to generate high-resolution sequences in a timely manner to assess treatment response. However, it is recognized that some institutions will be unable to implement the “ideal” MRI protocol. Therefore, a widely implementable 3T and 1.5T “minimal” protocol is provided. As such, the IPCG encourages the use of the same imaging protocol and MRI platform across the patients’ follow-up imaging time points. We acknowledge that many institutions utilize a single imaging protocol for all brain tumor etiologies. In this clinical context, these recommendations should not be viewed as being in conflict. The IPCG consensus recommendations build upon previously published imaging consensus guidelines that can be married into a BTIP compliant routine clinical imaging protocol.

## Conclusion

In summary, we have critically reviewed the application of MRI and PET in the setting of PCNSL and have described the results from an international survey of current imaging practice in this rare disease. This has guided the IPCG in developing and presenting here consensus recommendations for the imaging of PCNSL. These consensus imaging recommendations for MRI and PET Imaging are synergistic with BTIP protocols, but, notably differ by (1) utilizing volumetric imaging when possible for T1, T2, and FLAIR sequences, and (2) recommending CE-T2W-FLAIR sequences. Similar to BTIP metastasis recommendations, the IPCG recommends 3D TSE T1W pre- and post-contrast sequence be utilized. Additionally, IPCG DSC sequence parameters are synergistic with current consensus recommendations by Boxerman et al. Finally, whole body FDG-PET imaging is formally recommended as a metric for systemic staging evaluation. These recommendations have considered clinical feasibility, as determined from a recent clinical survey of current clinical imaging capabilities across multiple international health care facilities with experience in PCNSL management, and should help standardize consensus methods for PCNSL imaging in both clinical practice and in clinical

trials. This will facilitate future correlative studies to identify promising predictive and diagnostic imaging biomarkers in the context of clinical trials of new treatment strategies.

## Supplementary Material

Supplementary material is available at *Neuro-Oncology* online.

## Keywords

imaging | MRI | PCNSL | PET | primary central nervous system lymphoma

## Funding

Ramon F Barajas Jr: National Institutes of Health (NIH) National Cancer Institute (NCI) 1K08CA237809-01A1. Benjamin M Ellingson: American Cancer Society (ACS) Research Scholar Grant (RSG-15-003-01-CCE) UCLA SPORE in Brain Cancer (National Institutes of Health (NIH) National Cancer Institute (NCI) 1P50CA211015-01A1) National Institutes of Health (NIH) National Cancer Institute (NCI) 1R21CA223757-01. Leland S. Hu: National Institutes of Health (NIH) National Cancer Institute (NCI) U01CA220378; National Institutes of Health (NIH) National Cancer Institute (NCI) R01CA221938; National Institutes of Health (NIH) National Institute of Neurological Disorders and Stroke (NINDS) R21NS082609; Mayo Clinic Foundation.

## Acknowledgments

The first author thanks Bethany Barajas, MSN and David Pettersson MD for their helpful comments; the many clinical collaborators, including Joseph Anderson-Bussiere and Shannon Spruell, for their helpfulness; and the many wonderful patients

who selflessly contribute their time to undergo research medical imaging while confronting a deadly disease.

**Conflict of interest statement.** R.F.B.—No financial disclosures, grant funding: NIH/NCI 1K08CA237809-01A1. L.S.P.—no financial disclosures, no grant acknowledgment. N.A.—disclosure: speaker, consultant for Bayer Healthcare; C.P.F.—No conflicts or relevant grants for this manuscript; J.L.B.—no financial disclosures, no grants related to this paper. T.J.K.—financial disclosures: none relevant to neurooncology, consultant for and stock owner in SpineThera, no grant acknowledgments relevant. C.C.Q.—financial disclosures: C.C.Q. received grant support from Philips Healthcare and Blue Earth Diagnostics. B.M.E.—financial disclosures: B.M.E. is an advisor for Hoffman La-Roche, Siemens, Nativis, Medicenna, MedQIA, Bristol Meyers Squibb, Imaging Endpoints, VBL, and Agios Pharmaceuticals; B.M.E. is a Paid Consultant for Nativis, MedQIA, Siemens, Hoffman La-Roche, Imaging Endpoints, Medicenna, and Agios; B.M.E. received grant funding from Siemens, Agios, and Janssen; Grant funding: American Cancer Society (ACS) Research Scholar Grant (RSG-15-003-01-CCE), UCLA SPORE in Brain Cancer (NIH/NCI 1P50CA211015-01A1), and NIH/NCI 1R21CA223757-01. L.H.R.—financial disclosures: Department of Radiology Advanced Imaging Research Center Knight Cancer Institute Oregon Health & Science University. L.S.H.—Grant Funding: NS082609, CA221938, CA220378, Mayo Clinic Foundation; Precision Oncology Insights (co-founder); Imaging Biometrics (medical advisory board). All other authors declare no conflict of interest.

## References

- Ostrom QT, Gittleman H, Liao P, et al. CBTRUS Statistical Report: primary brain and other central nervous system tumors diagnosed in the United States in 2010–2014. *Neuro Oncol*. 2017;19(suppl\_5):v1–v88.
- Grommes C, DeAngelis LM. Primary CNS lymphoma. *J Clin Oncol*. 2017;35(21):2410–2418.
- Abrey LE, Batchelor TT, Ferreri AJ, et al.; International Primary CNS Lymphoma Collaborative Group. Report of an international workshop to standardize baseline evaluation and response criteria for primary CNS lymphoma. *J Clin Oncol*. 2005;23(22):5034–5043.
- Ellingson BM, Bendszus M, Boxerman J, et al.; Jumpstarting Brain Tumor Drug Development Coalition Imaging Standardization Steering Committee. Consensus recommendations for a standardized brain tumor imaging protocol in clinical trials. *Neuro Oncol*. 2015;17(9):1188–1198.
- Kaufmann TJ, Smits M, Boxerman J, et al. Consensus recommendations for a standardized brain tumor imaging protocol for clinical trials in brain metastases. *Neuro Oncol*. 2020;22(6):757–772.
- Boxerman JL, Quarles CC, Hu LS, et al.; Jumpstarting Brain Tumor Drug Development Coalition Imaging Standardization Steering Committee. Consensus recommendations for a dynamic susceptibility contrast MRI protocol for use in high-grade gliomas. *Neuro Oncol*. 2020;22(9):1262–1275.
- Fischer L, Koch A, Schlegel U, et al. Non-enhancing relapse of a primary CNS lymphoma with multiple diffusion-restricted lesions. *J Neurooncol*. 2011;102(1):163–166.
- Carlson BA. Rapidly progressive dementia caused by nonenhancing primary lymphoma of the central nervous system. *AJNR Am J Neuroradiol*. 1996;17(9):1695–1697.
- DeAngelis LM. Cerebral lymphoma presenting as a nonenhancing lesion on computed tomographic/magnetic resonance scan. *Ann Neurol*. 1993;33(3):308–311.
- Terae S, Ogata A. Nonenhancing primary central nervous system lymphoma. *Neuroradiology*. 1996;38(1):34–37.
- Bowden SG, Munger DM, Thiessen J, et al. The clinical heterogeneity of entirely nonenhancing CNS lymphoma: a case series. *CNS Oncol*. 2020;CNS67. doi:10.2217/cns-2020-0020.
- Mathews VP, Caldemeyer KS, Lowe MJ, Greenspan SL, Weber DM, Ulmer JL. Brain: gadolinium-enhanced fast fluid-attenuated inversion-recovery MR imaging. *Radiology*. 1999;211(1):257–263.
- Bristol-Myers S. A study of nivolumab in relapsed/refractory primary central nervous system lymphoma (PCNSL) and relapsed/refractory primary testicular lymphoma (PTL) (CheckMate 647). NCT:02857426. 2016. <https://clinicaltrials.gov/ct2/show/NCT02857426>. Accessed February 12, 2019.
- Matthias P. Study on pembrolizumab for recurrent primary central nervous system lymphoma (PCNSL). NCT:02779101. 2016. <https://clinicaltrials.gov/ct2/show/NCT02779101>. Accessed February 12, 2019.
- Korfel A. “Wonder drugs” in central nervous system lymphoma. *Transl Cancer Res*. 2017;S1158–S1162.
- Ambady P, Szidonya L, Firkins J, et al. Combination immunotherapy as a non-chemotherapy alternative for refractory or recurrent CNS lymphoma. *Leuk Lymphoma*. 2019;60(2):515–518.
- Ng S, Butzkueven H, Kalnins R, Rowe C. Prolonged interval between sentinel pseudotumoral demyelination and development of primary CNS lymphoma. *J Clin Neurosci*. 2007;14(11):1126–1129.
- Hu LS, Baxter LC, Smith KA, et al. Relative cerebral blood volume values to differentiate high-grade glioma recurrence from posttreatment radiation effect: direct correlation between image-guided tissue histopathology and localized dynamic susceptibility-weighted contrast-enhanced perfusion MR imaging measurements. *AJNR Am J Neuroradiol*. 2009;30(3):552–558.
- Barajas RF Jr, Chang JS, Segal MR, et al. Differentiation of recurrent glioblastoma multiforme from radiation necrosis after external beam radiation therapy with dynamic susceptibility-weighted contrast-enhanced perfusion MR imaging. *Radiology*. 2009;253(2):486–496.
- Tun HW, Johnston PB, DeAngelis LM, et al. Phase 1 study of pomalidomide and dexamethasone for relapsed/refractory primary CNS or vitreoretinal lymphoma. *Blood*. 2018;132(21):2240–2248.
- Rowley HA, Grant PE, Roberts TP. Diffusion MR imaging. Theory and applications. *Neuroimaging Clin N Am*. 1999;9(2):343–361.
- Guo AC, Cummings TJ, Dash RC, et al. Lymphomas and high-grade astrocytomas: comparison of water diffusibility and histologic characteristics. *Radiology*. 2002;224(1):177–183.
- Barajas RF Jr, Rubenstein JL, Chang JS, Hwang J, Cha S. Diffusion-weighted MR imaging derived apparent diffusion coefficient is predictive of clinical outcome in primary central nervous system lymphoma. *AJNR Am J Neuroradiol*. 2010;31(1):60–66.
- Valles FE, Perez-Valles CL, Regalado S, Barajas RF, Rubenstein JL, Cha S. Combined diffusion and perfusion MR imaging as biomarkers of prognosis in immunocompetent patients with primary central nervous system lymphoma. *AJNR Am J Neuroradiol*. 2013;34(1):35–40.
- Wieduwilt MJ, Valles F, Issa S, et al. Immunochemotherapy with intensive consolidation for primary CNS lymphoma: a pilot study and prognostic assessment by diffusion-weighted MRI. *Clin Cancer Res*. 2012;18(4):1146–1155.
- Mabray MC, Barajas RF, Villanueva-Meyer JE, et al. The combined performance of ADC, CSF CXC chemokine ligand 13, and CSF interleukin

- 10 in the diagnosis of central nervous system lymphoma. *AJNR Am J Neuroradiol.* 2016;37(1):74–79.
27. Hu LS, Eschbacher JM, Dueck AC, et al. Correlations between perfusion MR imaging cerebral blood volume, microvessel quantification, and clinical outcome using stereotactic analysis in recurrent high-grade glioma. *AJNR Am J Neuroradiol.* 2012;33(1):69–76.
  28. Barajas RF Jr, Phillips JJ, Parvataneni R, et al. Regional variation in histopathologic features of tumor specimens from treatment-naive glioblastoma correlates with anatomic and physiologic MR Imaging. *Neuro Oncol.* 2012;14(7):942–954.
  29. Sugahara T, Korogi Y, Shigematsu Y, et al. Perfusion-sensitive MRI of cerebral lymphomas: a preliminary report. *J Comput Assist Tomogr.* 1999;23(2):232–237.
  30. Takeuchi H, Matsuda K, Kitai R, Sato K, Kubota T. Angiogenesis in primary central nervous system lymphoma (PCNSL). *J Neurooncol.* 2007;84(2):141–145.
  31. Bao S, Watanabe Y, Takahashi H, et al. Differentiating between glioblastoma and primary CNS lymphoma using combined whole-tumor histogram analysis of the normalized cerebral blood volume and the apparent diffusion coefficient. *Magn Reson Med Sci.* 2019;18(1):53–61.
  32. Ferreri AJM, Calimeri T, Conte GM, et al. R-CHOP preceded by blood-brain barrier permeabilization with engineered tumor necrosis factor- $\alpha$  in primary CNS lymphoma. *Blood.* 2019;134(3):252–262.
  33. Anzalone N, Castellano A, Cadioli M, et al. Brain gliomas: multicenter standardized assessment of dynamic contrast-enhanced and dynamic susceptibility contrast MR images. *Radiology.* 2018;287(3):933–943.
  34. Lu S, Gao Q, Yu J, et al. Utility of dynamic contrast-enhanced magnetic resonance imaging for differentiating glioblastoma, primary central nervous system lymphoma and brain metastatic tumor. *Eur J Radiol.* 2016;85(10):1722–1727.
  35. Tofts PS, Brix G, Buckley DL, et al. Estimating kinetic parameters from dynamic contrast-enhanced t1-weighted MRI of a diffusable tracer: standardized quantities and symbols. *J Magn Reson Imaging.* 1999;10(3):223–232.
  36. Xi YB, Kang XW, Wang N, et al. Differentiation of primary central nervous system lymphoma from high-grade glioma and brain metastasis using arterial spin labeling and dynamic contrast-enhanced magnetic resonance imaging. *Eur J Radiol.* 2019;112:59–64.
  37. Younes A, Hilden P, Coiffier B, et al. International Working Group consensus response evaluation criteria in lymphoma (RECIL 2017). *Ann Oncol.* 2017;28(7):1436–1447.
  38. Malani R, Bhatia A, Wolfe J, Grommes C. Staging identifies non-CNS malignancies in a large cohort with newly diagnosed lymphomatous brain lesions. *Leuk Lymphoma.* 2019;60(9):2278–2282.
  39. Mohile NA, Deangelis LM, Abrey LE. The utility of body FDG PET in staging primary central nervous system lymphoma. *Neuro Oncol.* 2008;10(2):223–228.
  40. Makino K, Hirai T, Nakamura H, et al. Does adding FDG-PET to MRI improve the differentiation between primary cerebral lymphoma and glioblastoma? Observer performance study. *Ann Nucl Med.* 2011;25(6):432–438.
  41. Krebs S, Wolfe J, Mellinghoff I, Grommes C, Schoder H. Prognostic value of FDG-PET/CT in recurrent/refractory CNS lymphoma receiving Ibrutinib-based therapies. *Eur J Nucl Med Mol Imaging.* 2019;46(Suppl. 1): S260.
  42. Rosenfeld SS, Hoffman JM, Coleman RE, Glantz MJ, Hanson MW, Schold SC. Studies of primary central nervous system lymphoma with fluorine-18-fluorodeoxyglucose positron emission tomography. *J Nucl Med.* 1992;33(4):532–536.
  43. Fukuoka H, Hirai T, Okuda T, et al. Comparison of the added value of contrast-enhanced 3D fluid-attenuated inversion recovery and magnetization-prepared rapid acquisition of gradient echo sequences in relation to conventional postcontrast T1-weighted images for the evaluation of leptomeningeal diseases at 3T. *AJNR Am J Neuroradiol.* 2010;31(5):868–873.
  44. Padhani AR, Liu G, Koh DM, et al. Diffusion-weighted magnetic resonance imaging as a cancer biomarker: consensus and recommendations. *Neoplasia.* 2009;11(2):102–125.
  45. Welker K, Boxerman J, Kalnin A, Kaufmann T, Shiroishi M, Wintermark M; American Society of Functional Neuroradiology MR Perfusion Standards and Practice Subcommittee of the ASFNR Clinical Practice Committee. ASFNR recommendations for clinical performance of MR dynamic susceptibility contrast perfusion imaging of the brain. *AJNR Am J Neuroradiol.* 2015;36(6):E41–E51.
  46. Patel P, Baradaran H, Delgado D, et al. MR perfusion-weighted imaging in the evaluation of high-grade gliomas after treatment: a systematic review and meta-analysis. *Neuro Oncol.* 2017;19(1):118–127.
  47. Boxerman JL, Hamberg LM, Rosen BR, Weisskoff RM. MR contrast due to intravascular magnetic susceptibility perturbations. *Magn Reson Med.* 1995;34(4):555–566.
  48. Boxerman JL, Schmainda KM, Weisskoff RM. Relative cerebral blood volume maps corrected for contrast agent extravasation significantly correlate with glioma tumor grade, whereas uncorrected maps do not. *AJNR Am J Neuroradiol.* 2006;27(4):859–867.
  49. Schmainda KM, Prah MA, Hu LS, et al. Moving toward a consensus DSC-MRI protocol: validation of a low-flip angle single-dose option as a reference standard for brain tumors. *AJNR Am J Neuroradiol.* 2019;40(4):626–633.
  50. Hu LS, Kelm Z, Korfiatis P, et al. Impact of software modeling on the accuracy of perfusion MRI in Glioma. *AJNR Am J Neuroradiol.* 2015;36(12):2242–2249.
  51. Boxerman JL, Prah DE, Paulson ES, Machan JT, Bedekar D, Schmainda KM. The role of preload and leakage correction in gadolinium-based cerebral blood volume estimation determined by comparison with MION as a criterion standard. *AJNR Am J Neuroradiol.* 2012;33(6):1081–1087.
  52. Leu K, Boxerman JL, Ellingson BM. Effects of MRI protocol parameters, preload injection dose, fractionation strategies, and leakage correction algorithms on the fidelity of dynamic-susceptibility contrast MRI estimates of relative cerebral blood volume in gliomas. *AJNR Am J Neuroradiol.* 2017;38(3):478–484.